ON THE LAW OF STAR FORMATION IN DISK GALAXIES

MICHAEL A. DOPITA AND STUART D. RYDER[1]
Mount Stromlo and Siding Spring Observatories, Institute of Advanced Studies, Australian National University,
Private Bag, Weston Creek P.O., ACT 2611, Australia
Received 1993 August 11; accepted 1994 January 18

ABSTRACT

The observational relationship between the stellar surface brightness and the surface brightness in Hα in galactic disks is shown to be determined by the law of star formation in disk galaxies. Assuming the rate of star formation to take a generalized Schmidt power-law form dependent on both the total local matter surface density, σ_T, and the gas surface density, σ_g; $d\sigma_*/dt = \epsilon \sigma_T^n \sigma_g^m$, we find that the observations constrain $(n + m) > 1$, and that the best fit is obtained for $1.5 < (n + m) < 2.5$. Both a Schmidt Law of the form $d\sigma_*/dt = \epsilon \sigma_g$, and a star-formation law of the form $d\sigma_*/dt = \epsilon \Omega \sigma_g$, where Ω is the angular velocity at the radial point considered, seem to be excluded by observations. The observed scatter in the stellar surface brightness versus Hα surface brightness relationship can be interpreted as a scatter in the ratio of galaxian age to star-formation efficiency; younger galaxies being more gas-rich, and currently more active in forming stars. Finally, we discuss particular forms of the Schmidt Law given by theory. We show that a model having $n = 1/3$ and $m = 5/3$, which gives a particularly good fit to the observations, follows as a consequence of stochastic self-regulating star formation moderated by cloud-cloud interactions in the disk potential, and by the energetic processes associated with the formation of massive stars. This model explicitly includes the secular evolution of the vertical structure of the gaseous and stellar components of galactic disks, and the effect of the galaxian potential.

Subject headings: galaxies: evolution — galaxies: photometry — galaxies: spiral — galaxies: stellar content — stars: formation

1. INTRODUCTION

The structure and evolution of spiral galaxies remain a key subject for study in modern astrophysics, since results in this area have an impact in so many different areas and subdisciplines. In particular, an understanding of the physical processes which control star formation in galactic disks is vital. Over the years, many evolutionary models have been proposed, each of which may be capable of reproducing many of the observed characteristics of disk galaxies, including our own Milky Way. However, the main defect of such models must surely lie in their lack of uniqueness, resulting in part from a lack of adequate observational constraints on those models. For instance, we can presently determine reasonably reliable chemical compositions for individual stars only if they are located in the solar neighborhood or in the Magellanic Clouds. The dynamical characteristics, the chemical abundances and the chemical abundance distribution of the long-lived stars in the solar neighborhood are the most often-used constraints on the various theoretical galaxy evolution scenarios. But how can we be sure that the solar neighborhood represents a typical region of this or any other galaxy? On a Galaxy-wide basis, even such fundamental parameters as the mass of the galaxy, the distance of the Sun from the Galactic center, the exponential scale length of the stellar distribution, the distribution of the atomic and molecular gas, and the size of the abundance gradients in different elements, remain unacceptably uncertain (see reviews by Rana 1991, Combes 1991, and Fich & Tremaine 1991).

Fortunately, a large number of galaxies of all types are located close enough to the Milky Way to present a significant angular size on the sky, and for which it is theoretically possible to determine the radial variation of such parameters as the surface density of old and young stars, star-forming activity, neutral and ionized gas, radio continuum emission, and chemical abundance gradients. Indeed, some of the best examples are so close as to be simply too large for the current generation of high-sensitivity, high-resolution instruments such as CCDs and radio aperture synthesis arrays. Although surface photometry and radio studies are available for a number of individual objects, what is really needed are consistent *homogeneous* surveys of such galaxies to procure fundamental observational constraints for the models, an example of which is the Palomar-Groningen survey of northern spiral galaxies (Wevers, van der Kruit, & Allen 1986).

We have recently obtained photometric CCD imaging data for 34 nearby southern spiral galaxies covering the full range in Hubble sub-type (Ryder 1993; Ryder & Dopita 1993). Ryder & Dopita (1994, hereafter Paper I) performed surface photometry of the I, V, and spectrally pure Hα images, from which the radial run in surface density of the old stars, intermediate-age stars, and recently formed massive stars respectively could be computed. A striking correlation was discovered between the surface brightness in the I-band (which measures the surface density of the old, low-mass stars) and in Hα (which measures the current formation rate of massive stars having $M \gtrsim 10\ M_\odot$; Kennicut 1983).

In this paper, we investigate what such a correlation implies about the form of the star-formation law in disk galaxies; a key parameter in our understanding of the nature of galactic evolution.

[1] Postal address: Department of Physics and Astronomy, University of Alabama, Box 870324, Tuscaloosa, AL 35487-0324.

163

2. CALIBRATION OF THE SURFACE BRIGHTNESS RELATIONSHIP

The existence of an I-band versus Hα surface brightness correlation, the slope of which is independent of galaxian type and galaxy luminosity, is powerful evidence in support of a model in which star formation is controlled by physical mechanisms of a local rather than global nature. However, the form of the correlation presented in Paper I does not lend itself very readily to direct physical interpretation. In this section, we convert the observed quantities to more obvious parameters of disk surface mass density and formation rate of massive stars.

2.1. The Mass-To-Light Ratio

In this thesis, Buchhorn (1992) examined the Tully-Fisher relationship for a large number of spiral galaxies as part of a study in search of the Great Attractor. He found that the mass-to-light (M/L) ratio remained remarkably constant from one galaxy to another, based on a maximal disk model of the rotation curve. The apparent M/L ratio is somewhat higher for galaxies with $i > 60°$. For the galaxies with $i < 60°$, $\langle M/L_I \rangle = 4.2$, with a standard deviation of ± 1.3. Since our sample is chosen to have $i < 60°$ in general, we have adopted this value to convert the I surface brightness into a surface mass density.

2.2. The Hα Surface Brightness

If we assume that the interstellar medium (ISM) in a Galaxy is capable of absorbing all of the UV photons produced by high-mass ($M > 10 M_\odot$) stars, then the Hα flux is a direct measure of the surface area of the OB stars which are currently alive. This assumption appears to be valid in that very few H II regions display the spectral characteristics of an optically thin nebulosity (McCall, Rybski, & Shields 1985; Dopita & Evans 1986; Belley & Roy 1992). Fitting the results of Wilson (1983) to a simple power law, we find that the mean rate of production of UV photons by a single star during its lifetime, S_*, can be described by a simple function of the mass:

$$\ln S_* = 92.07 + 8.6353 \ln (M/M_\odot) - 0.8009 [\ln (M/M_\odot)]^2 .$$
(2.1)

Each of these photons produces an ionization, and from nebular theory, $45 \pm 3\%$ of these ionizations produce an Hα photon on recombination. The relationship between the mass of the star and the Hα flux which it produces in its surrounding H II region is therefore:

$$\ln S_{\mathrm{H}\alpha} = -12.58 + 8.6353 \ln (M/M_\odot) - 0.8009 [\ln (M/M_\odot)]^2 .$$
(2.2)

This flux is produced during the lifetime of the star. The main-sequence lifetime can be represented by the following equations estimated using the calculations of Chiosi & Maeder (1986), Maeder (1983, 1987), and Maeder & Meynet (1987):

$$\tau_{\mathrm{H}} = 4.53(M/40\ M_\odot)^{-0.97}\ \mathrm{Myr} \quad M \le 42\ M_\odot$$
$$\tau_{\mathrm{H}} = 4.53(M/40\ M_\odot)^{-0.43}\ \mathrm{Myr} \quad M > 42\ M_\odot ,$$
(2.3)

and the helium-burning lifetime is given by

$$\tau_{\mathrm{He}} = 0.856(M/40\ M_\odot)^{-0.97}\ \mathrm{Myr} \quad M \le 42\ M_\odot$$
$$\tau_{\mathrm{He}} = 0.78\ \mathrm{Myr} \quad\quad\quad\quad\quad\quad M > 42\ M_\odot,$$
(2.4)

provided that stellar mass-loss does not terminate either the hydrogen-burning or helium burning phases.

We adopt the initial mass function (IMF) used by Kennicutt (1983):

$$\psi(M) = M^{-1.4} \quad 0.1\ M_\odot \le M < 1\ M_\odot$$
$$\psi(M) = M^{-2.5} \quad 1.0\ M_\odot \le M \le 100\ M_\odot$$
(2.5)

where $\psi(M)$ is the number of stars per unit mass interval. This is a power-law approximation to the Miller & Scalo (1979) solar neighborhood IMF. With these calibrations, we find that a luminosity of $1.0\ L_\odot\ \mathrm{pc}^{-2}$ in Hα is equivalent to a birthrate for massive stars ($M > 10\ M_\odot$) of $3.05\ M_\odot\ \mathrm{pc}^{-2}\ \mathrm{Gyr}^{-1}$, and a total birthrate (over all stellar masses) of $22.93\ M_\odot\ \mathrm{pc}^{-2}\ \mathrm{Gyr}^{-1}$. These figures are in good agreement with the Kennicutt (1983) values of $3\ M_\odot\ \mathrm{pc}^{-2}\ \mathrm{Gyr}^{-1}$ and $18\ M_\odot\ \mathrm{pc}^{-2}\ \mathrm{Gyr}^{-1}$, respectively. Clearly, the first of these figures is the much more reliable of the two, since the low-mass IMF is poorly defined.

These expressions have been used to calibrate the observed relationship between mean stellar surface density and surface density of the rate of star formation, shown in Figure 1. Here we have plotted both the Hα luminosity density and the equivalent specific star-formation rate for massive ($M > 10\ M_\odot$) stars on the vertical axis, and the I-band surface luminosity and the stellar surface density on the horizontal axis. Paper I shows that the loci of Hα versus I plotted for each of the 34 galaxies exhibit remarkably similar slopes, and furthermore, each one possesses a vertical offset which scales in accordance with their mean H I surface density, in the sense that gas-rich galaxies have a higher Hα surface brightness at a given surface mass density than gas-poor ones. The light dots in Figure 1 represent the values determined at each sampled radius from the 34 individual galaxies, after scaling all galaxies to a common mean H I surface density $\sim 5\ M_\odot\ \mathrm{pc}^{-2}$. The filled circles show the resultant mean relationship after binning in stellar surface density, covering the range where we have enough photometric points, and where the measurements are neither severely affected by bulge components on the one hand, or by uncertain sky subtraction on the other.

3. THE OBSERVATIONAL SCHMIDT LAW FOR STAR FORMATION

3.1. A Generalized Schmidt Law

As Silk (1985) pointed out, the essential ingredients of a star-formation theory are the IMF, the star-formation efficiency, and the rate of star formation. Most models of galactic evolution (Audouze & Tinsley 1977; Vader & de Jong 1981) have tended to assume a constant IMF and to reduce the star-formation problem to a simple "prescription" of the rate as a power law of the local H I gas density (Schmidt 1959), or of the H I surface density (Sanduleak 1969; Hamajima & Tosa 1975). However, it has become apparent that the molecular component of the gas can exceed the atomic contribution by a considerable margin (e.g., Young & Scoville 1982; Scoville & Young 1983; Sanders, Solomon, & Scoville 1984), and a better correlation is claimed between the total gas surface density and star-formation rate (Talbot 1980; DeGioia-Eastwood et al. 1984; Kennicutt 1989), and this has been used in the more recent models of galactic chemical evolution. However, the question of an appropriate conversion factor to use to transform observed CO luminosities into molecular hydrogen content has remained a key source of uncertainty (e.g., Maloney & Black 1988; Israel 1988; Dickman, Snell, & Schloerb 1986).
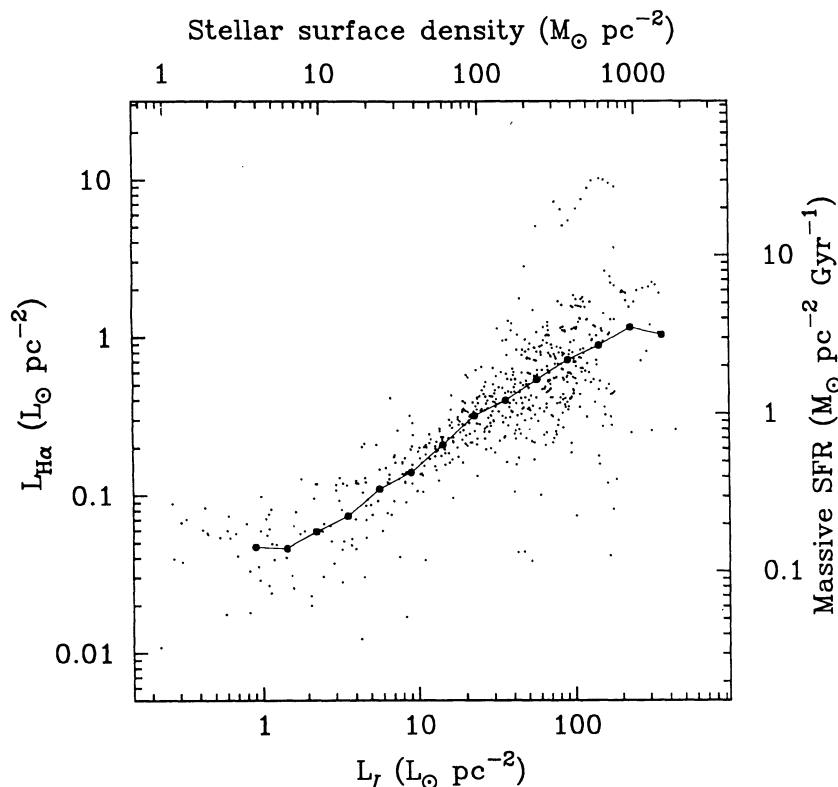
FIG. 1.—Observational correlation between the *I*-band surface brightness (or equivalently, the stellar surface density) and the Hα surface luminosity (or equivalently, the rate of formation of massive stars). The small dots represent the observed points for the full sample of galaxies observed, after applying the offset in the vertical direction (Ryder & Dopita 1994). The line connecting the large dots represents our adopted mean relationship.

Direct observational tests of Schmidt Laws are not a straightforward matter. As Madore (1977) pointed out, the best we can do is to compare the recent products of star formation (young stars, H II regions, etc.) with the gas that remains, rather than with the gas that may have been available at the time of formation. Wyse (1986) makes the point that the relative constancy of the H I surface density over the star-forming disk makes the predicted SFR rather insensitive to the power of the Schmidt Law adopted, and thus it is not surprising that a wide range of indices can be considered to be compatible with the observations. Struck-Marcell (1991) has argued with the assistance of hydrodynamical considerations that radial gas flows must operate in order to balance gas consumption by star formation. If this is the case, then it would tend to further disguise the actual form of the Schmidt Law (if indeed such a law applies).

Bearing these points in mind, and noting that we lack data on the radial gas distributions for the bulk of our sample, we choose to adopt a particular form of the Schmidt Law in our modeling, let the model evolve for a Hubble time, and test whether it can then account for the observed *I*: Hα correlation. By this means we hope to place stronger observational constraints on the form of the Schmidt Law which may apply in real galaxies.

Dopita (1985, 1990) has argued that a simple Schmidt Law dependent only on the gas density is inappropriate, since the properties of the gas clouds are determined by the local environment, which depends in turn on the total surface density of matter. For the purposes of the following discussion, we adopt a "compound" Schmidt-type law in terms of the total disk surface density σ_T, and the gas surface density σ_g, of the form:

$$d\sigma_*/dt = \epsilon(\sigma_T/100\ M_\odot\ pc^{-2})^n(\sigma_g/100\ M_\odot\ pc^{-2})^m\ , \quad (3.1)$$

where ϵ represents an efficiency term, and n and m are arbitrary powers. The "classical" Schmidt Law then has $n = 0$ and $m = 2$. In practice, the efficiency factor may not be a constant, but may also be driven by collisionally enhanced star formation during infall, or by structural evolution of the galactic disk as may be caused, for example, by stellar diffusion (Spitzer & Schwarzschild 1951, 1953; Wielen 1977; Villumsen 1985). However, for the purposes of the following discussion, we assume this term to be a constant during the lifetime of the disk.

Considerations of the gravitational stability of disks have led to the suggestion that disks may form stars in such a way as to self-regulate their Toomre parameter. In galaxies with a flat rotation curve, this then leads to the particular form of Schmidt Law (Larson 1988; Silk 1988; Wyse & Silk 1989):

$$d\sigma_*/dt = \epsilon\Omega\sigma_g\ . \quad (3.2)$$

In this case, the star formation law is coupled to the global mass distribution in the galaxy. Such a star-formation law can be regarded as formally equivalent to equation (3.1), but with a radius-dependent efficiency term. For the purposes of this section, we restrict consideration of the form of the star-formation law to that of equation (3.1). However, we discuss in the following sections the derivation of equation (3.2), and the extent to which our data can be regarded as consistent with this equation.

3.2. A Disk Evolution Model

The current gas content of any part of the galactic disk will depend on the infall history and the total surface density accumulated throughout time, moderated by the locking up of gas through low-mass star formation. High-mass star formation also locks away a portion of the gas through stellar remnants

(neutron stars, black holes, and the like). Intermediate mass star formation initially reduces the amount of gas, but as these stars evolve they can liberate gas back into the ISM in the form of winds and planetary nebulae ejection. These processes may occur over a period of time which is quite similar to the gas infall, or gas depletion timescales. In order to compute the evolution of the gas surface density we must therefore allow for all of these processes, assuming an IMF given by equation (2.5), and a generalized star formation law of the form given by equation (3.1). In order to do this we have used a modified version of the code described by Dopita (1990) and Russell & Dopita (1992).

The mass infall timescale, considered by a variety of authors (Larson 1972; Searle 1972; Lynden-Bell 1975; Chiosi 1980; Vader & de Jong 1981; Lacey & Fall 1983, 1985; Lacy 1984), is loosely constrained by the free-fall collapse timescale:

$$\tau_{ff} = 1.65(R_{100}^3/M_{11})^{1/2} \text{ Gyr} , \qquad (3.3)$$

where the radius over which the gas is initially distributed, R_{100}, is measured in units of 100 kpc, and the total galaxian mass, M_{11}, is measured in units of $10^{11} M_\odot$.

The mass infall is generally assumed to be an exponentially decreasing function of time, although Chiosi (1980) allows in addition a low level of continuous inflow. In order to come close to fitting the metallicity distribution of GK-dwarfs in the local disk through this process alone, long infall timescales are indicated for our Galaxy, of order 3–6 Gyr. Such long timescales require infall from very large initial radii. Since the mass of our Galaxy is about $4 \times 10^{11} M_\odot$, the proto-Galaxy is required to have had a diameter of order 300–600 kpc in this model. Such a value is not absolutely excluded, but it does seem uncomfortably large.

In our model, we have assumed an exponentially decreasing mass infall with an infall timescale of 2.5 Gyr estimated on the basis of equation (3.3). Clearly, the infall timescale depends on the mass of the galaxy, and this will have a direct influence on the final gas content, low mass galaxies being relatively more gas-rich. There is also some likelihood that the infall timescale is a function of radius within a galaxy, since we might expect material in the outer parts of galaxies to be derived from larger proto-galactic radii. However, we choose to ignore these complications at this stage.

The stellar lifetime is taken as (Iben 1987):

$$\tau_* = 2.64(M/M_\odot)^{-2.16} \text{ Gyr} , \quad 2.3 \, M_\odot < M < 10 \, M_\odot$$

$$\tau_* = 11.0(M/M_\odot)^{-3.5} \text{ Gyr} , \qquad M \leq 2.3 \, M_\odot , \quad (3.4)$$

while above $10 \, M_\odot$, equations (2.3) and (2.4) are assumed to apply. For the low- and intermediate-mass stars to which equation (3.4) applies, the vast majority of the mass-loss occurs in the giant and asymptotic giant branch phases of evolution. Thus, these equations tell us the time over which gas is stored in stars prior to its return to the interstellar medium.

The mass of stellar remnants, M_{rem}, assumed to be left behind after the death of a single star of any mass, is given by the following semi-empirical equations based on the theoretical evolutionary computations of Vassiliadis (1992), Iben & Tutukov (1985), and Arnett (1978):

$$(M_{rem}/M_\odot) = 0.515\{1 + 0.147(M/M_\odot)\} \quad M < 8 \, M_\odot$$

$$(M_{rem}/M_\odot) = 1.37 \qquad\qquad 8 \, M_\odot \leq M \leq 12 \, M_\odot \quad (3.5)$$

$$(M_{rem}/M_\odot) = 1.42 + 0.01\{(M-12)/M_\odot\} \quad M > 12 \, M_\odot .$$

With these prescriptions, we have attempted to derive, as a function of total surface mass density, the evolution of the rate of formation of massive stars per unit area in the disk (or equivalently, the surface brightness in Hα), and the evolution of the surface density of low-mass stars (or equivalently, the surface brightness in the I-band).

3.3. *Results*

We computed the temporal evolution of a set of galaxian disks without radial flow, covering the full range of surface densities liable to be encountered in star-forming zones of real disks: $8.0 \, M_\odot \text{ pc}^{-2}$, up to $2048 \, M_\odot \text{ pc}^{-2}$. The indices m and n in the generalized Schmidt star formation law (eq. [3.1]) were taken to be free variables. The efficiency factor ϵ was adjusted so as to produce the observed stellar and gaseous surface densities of our solar neighborhood at the current epoch.

This calibration with respect to the solar neighborhood is less certain than one might expect, since there is still considerable uncertainty about the total mass density, and the fraction of the gas which is in the molecular form. Here, we adopt the value estimated by Bahcall (1984) for the total mass surface density σ_T in the solar neighborhood. This was obtained by consideration of the vertical force measured locally, giving $\sigma_T = 67 \, M_\odot \text{ pc}^{-2}$. Estimates given in the literature range from 45 up to nearly $100 \, M_\odot \text{ pc}^{-2}$. Dynamical arguments based on the local rotation velocities require at least $54 \, M_\odot \text{ pc}^{-2}$ (Bahcall 1984). The total H I column density can be accurately determined from H I surveys in the directions of the north and south Galactic poles. From these, Mathewson (1992) has determined $N_{HI} = (0.7 \pm 0.1) \times 10^{21} \text{ cm}^{-2}$, which translates to a surface density of $7.6 \pm 0.8 \, M_\odot \text{ pc}^{-2}$ in the atomic component, taking the helium abundance in the solar neighborhood to be 0.102 by number with respect to hydrogen (Anders & Grevesse 1989). This is significantly higher than earlier estimates by Gordon & Burton (1976), Burton & Gordon (1978), and Blitz, Fich, & Kulkarni (1983), but they did not have the advantage of having the results of a deep southern H I survey. Locally, the $H_2/H I$ ratio is estimated by Rana (1991) to be 0.63, on the basis of a survey of the current literature. The mean value for the solar circle is almost certainly higher than this, since it is now known from EUV surveys that the Sun sits in a particularly low-density region in the ISM. In what follows, we assume that the molecular component has a mean surface density ∼0.8 of the H I at the solar circle. Thus, the total gas content is taken to be ∼0.8 of the H I at the solar circle. Thus, the total gas content is taken to be ∼$13.5 \pm 3.0 \, M_\odot \text{ pc}^{-2}$ locally.

The current estimates for the disk age have recently been reviewed by Cowan, Thielemann, & Truran (1991). Together, ages derived by nucleochronology and chemical evolution define a disk age in the range 13–15 Gyr, allowing for infall, although methods based on the white dwarf cooling timescales give 7–11 Gyr. In part, this apparent discrepancy may be due to the infall process itself, since for reasonable infall timescales ∼2–3 Gyr, the peak disk star-formation rate occurs after about 4 Gyr. We adopt a disk infall timescale of 2.5 Gyr, and total disk age of 13 Gyr, for the purpose of these calculations.

In Figure 2, we show the evolutionary history of the solar neighborhood, for the "classical" set of Schmidt Law indices $n = 0$; $m = 2$. However, the general evolution would appear very similar for another choice of star formation parameters.

For any choice of star formation parameters, a gas depletion timescale, τ_{dep}, can be defined in terms of the initial rate of gas
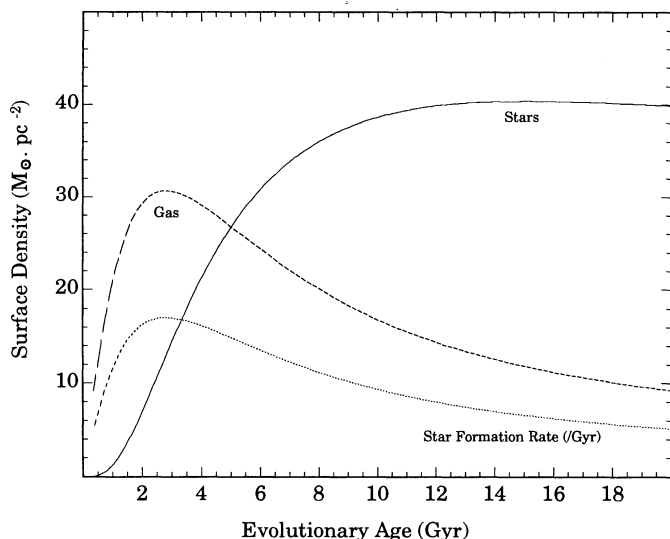
Fig. 2.—Evolution of the solar neighborhood according to the model described in the text for the "classical" Schmidt law having index $m = 2$. Note the initial increase in star forming activity and gas content resulting from infall. On this model, the surface mass density of visible stars reaches a maximum at about 15 Gyr, after which star formation is mostly maintained by gas supply from dying stars. The effective gas depletion timescale increases with age, which removes many of the problems associated with the fact that many galaxies seem to consume their gas supply on timescales which are short compared with their age (Kennicutt 1983).

consumption by high-mass star formation:

$$\tau_{dep} = \sigma_g / \{F \, d\sigma_* / dt\} \, , \qquad (3.6)$$

where σ_g is the instantaneous surface density of gas in the disk (in $M_\odot \, pc^{-2}$), $d\sigma_* / dt$ is the rate of star formation per unit area (in units of $M_\odot \, pc^{-2} \, yr^{-1}$), and F is the fraction of this star formation which is not returned promptly to the ISM through the various mass-loss processes. This fraction is calculated in the galactic evolution model through equations (2.3), (2.4), (3.4), and (3.5). Table 1 gives the initial gas depletion timescales required by various star formation laws in order to reproduce the solar neighborhood parameters after 13 Gyr of evolution. In general, higher indices in the Schmidt Law give a more rapid burst of star formation, and a correspondingly shorter initial gas depletion timescale.

In Figures 3a–3c, we show the computed relation between stellar surface density in units of $M_\odot \, pc^{-2}$ and the surface

TABLE 1

THE GAS DEPLETION TIMESCALES
REQUIRED TO FIT SOLAR NEIGHBORHOOD
PARAMETERS AS A FUNCTION OF THE
SCHMIDT LAW INDICES

SCHMIDT LAW INDICES		τ_{dep} (Gyr)
n	m	
0.0	1.0	5.204
0.0	1.5	3.151
0.0	2.0	1.846
0.5	1.0	5.039
0.5	1.5	3.033
0.5	2.0	1.995
1.0	1.0	4.848
1.0	1.5	2.917
1.0	2.0	1.945

brightness in Hα in units of $L_\odot \, pc^{-2}$ after 13 Gyr of evolution, for models with the various Schmidt Laws of Table 1. The fact that the computed curves lie close to the observed points suggests that the normalization with respect to the solar neighborhood is quite good.

All these curves, with the exception of the case $n = 0$; $m = 1$ have a characteristic S-shape. At low surface mass density, the star formation rate is determined by the amount of gas present, and very little gas has been converted into stars even up to the present day. As a consequence the slope in the observed relation is unity. By contrast, at very high surface mass density, effectively all of the gas initially present has been consumed into stars. The current star formation rate is determined by the supply of gas recycled by old, dying stars. This is determined by the total stellar mass surface density, and thus the slope in the relation is once again unity. Between these gas-dominated and star-dominated limits the slope is shallower.

The comparison between the theoretical and observed relationships, and other considerations, allow us to place limits on the allowable values of n and m. For example, all models in which $(n + m) < 1$ are excluded, since in these the slope of the theoretical relationship is too steep, and indeed could become greater than unity, on average. These are also excluded on the basis of observed abundance gradients. Abundances are observed to decrease toward the outer parts of galaxies. Model galaxies with $(n + m) < 1$ become more gas-dominated in the inner portion, and so have an outwardly increasing abundance gradient.

The case $n = 0$; $m = 1$ is a critical one. In this case, the gas depletion timescale, and consequently the gas fraction at all parts of the galaxy, is a constant. As a result, this model has a zero abundance gradient at all times, but the chemical abundances steadily increase with time. Models in which m is much greater than unity rapidly consume their gas supply and move to the star-dominated limit. This case is excluded by observation, since the observed slope of the star formation rate versus stellar surface density relation is less than unity, whereas these models predict a slope of unity.

The slope of the observational relation, the existence of abundance gradients, and the fact that gas fractions are observed to decrease towards the centers of galaxies (Bosma 1978; Wevers 1984), all tell us that disk galaxies are observed today in the transition between gas-dominated and star-dominated phases, and so intermediate values of $(n + m)$ are favored. The best fit between theory and observation is obtained in the approximate range $1.5 < (n + m) < 2.5$. The case $n = 0.5$; $m = 1$ is particularly good.

In Figure 4 we plot the full evolution for the "classical" Schmidt Law case $n = 0$; $m = 2$. Evolutionary trajectories on the stellar surface density versus Hα surface luminosity diagram are plotted for a set of total matter surface densities between 8 and 2048 $M_\odot \, pc^{-2}$. In addition, isochrones for a set of initial gas depletion timescales at solar neighborhood surface density (67 $M_\odot \, pc^{-2}$) are also plotted. For the case $n = 0$; $m = 2$, the observations are best fitted by a normalized disk age of $t/\tau_{dep} = 7.0 \pm 0.7$. This corresponds to a mean disk age of ~ 13 Gyr, as might have been expected by the normalization to the solar neighborhood. However, this result is not necessarily guaranteed, since the constant of proportionality between the star formation rate and the Hα surface luminosity is a sensitive function of the assumed IMF. The fact that these ages do agree is an indication that the IMF given in equation (2.5) is in fact quite a good model.
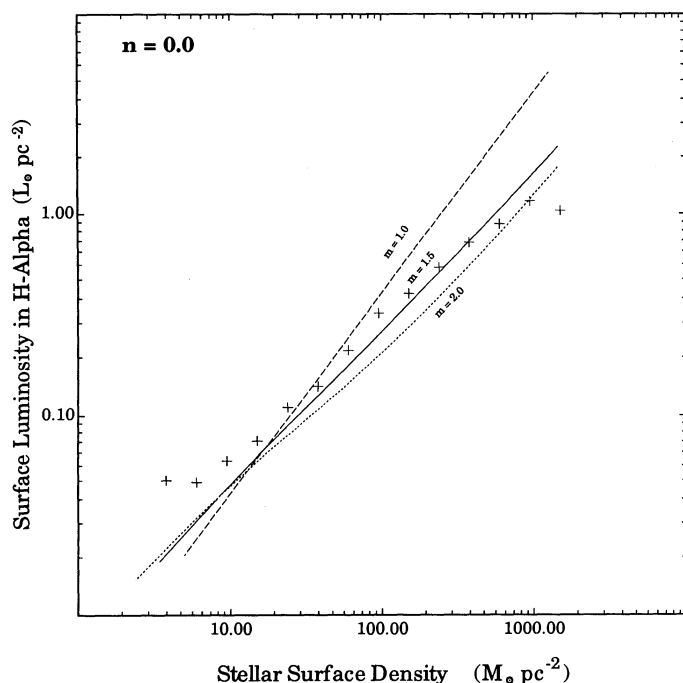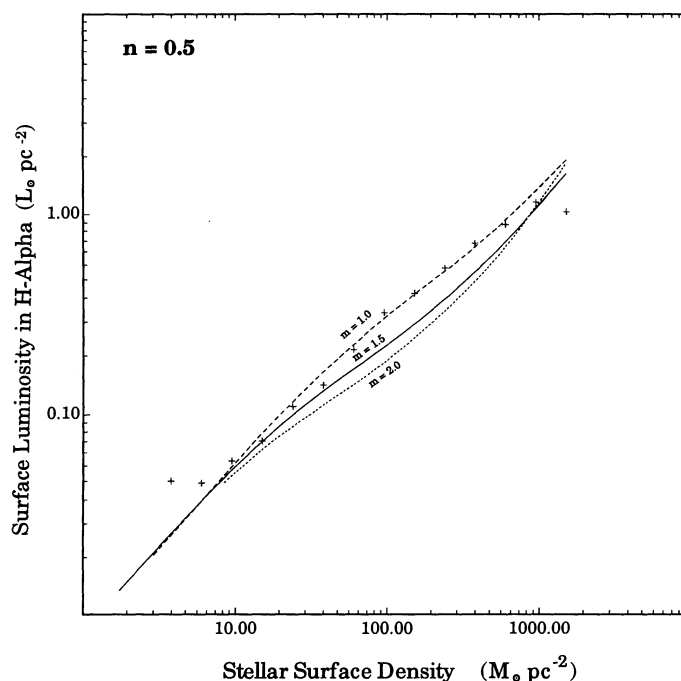
FIG. 3a

FIG. 3b
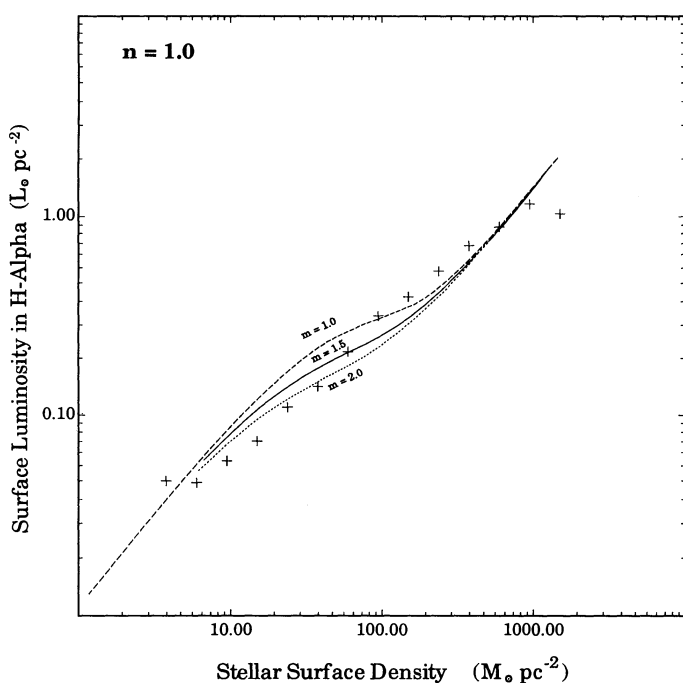

FIG. 3c

FIG. 3.—13 Gyr isochrones for various star formation laws are plotted with the observed points on the stellar surface density vs. Hα surface luminosity plot. The three plots show the effect of changing the Schmidt Law index on total surface density for the cases (a) $n = 0$, (b) $n = 0.5$, and (c) $n = 1.0$, respectively.

The zero-point offset in the base star formation rate between individual galaxies, which can amount to as much as 2.5 magnitudes in the Hα surface brightness (Paper I), can easily be understood on the basis of Figure 4. The position of any galactic disk on this diagram is determined by its normal-ized disk age. This parameter measures the *ratio* between the physical age of the galactic disk, and the star formation efficiency which characterizes that particular galactic disk. If all disk galaxies are the same age, then the S0 galaxies have disks which are characterized by a high efficiency of star formation. If, on the other hand, the star formation efficiency is a universal parameter of galactic disks, the Sd, Sm, and Irr-type galaxies must be physically younger.

Since the position of the isochrones on Figure 4 are such a weak function of the assumed disk age, we can use the observations of individual galaxies to determine on which isochrone they lie, and so estimate the disk age with respect to that of the solar neighborhood. We will call this the "star formation age" of the disk. The values so estimated are given in column (4) of Table 2. Columns (2) and (3) are, respectively, the exponential scale length of the disk in the *I*-band (Paper I), and the mean H I surface density, obtained by dividing the total H I gas content from the Reif et al. (1982) survey by the area of the galaxy out to the Holmberg radius, taken from de Vaucouleurs et al. (1991). The meaning of the other columns in Table 2 is explained in § 4.1, below. For some objects, the "star formation age" is uniquely determined throughout the disk. Others, on the other hand, show a continuous variation, and for these only the range can be given. A few objects show more than one distinct age. In these cases the various ages found are listed individually. These objects are of considerable intrinsic interest, since they suggest either that there have been a number of discrete episodes of accretion, or else that some local parameter has abruptly changed, leading to a markedly different star formation efficiency.

Since the overall level of star formation in a galaxy is set by the isochrone on which it lies, our star formation age parameter, τ_{sf}, is very closely related to the magnitude offset used in Paper I to overlay the different galaxies on the Hα surface luminosity versus *I*-band surface luminosity diagram (cf. Fig. 1). The relationship between the two parameters is well fit by
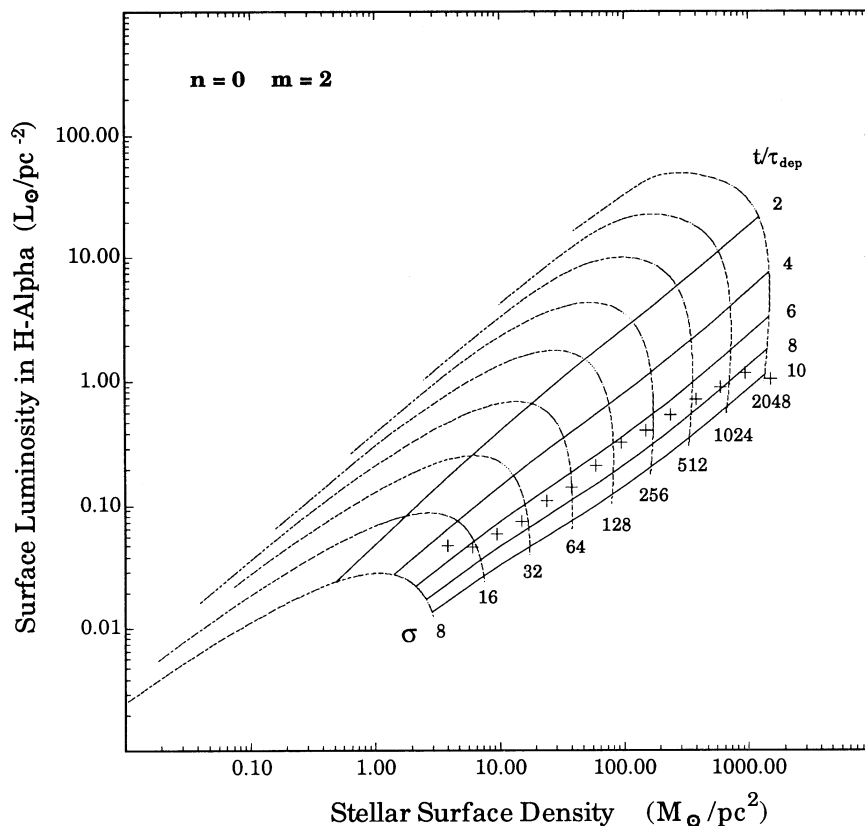
FIG. 4.—Full evolution of a model galactic disk described in the text on the stellar surface density vs. Hα surface luminosity plot. This has star formation following a "classical" Schmidt law with indices $n = 0$ and $m = 2$. Isochrones are given for a set of ages expressed in terms of the initial gas depletion timescale, and the trajectories followed by a set of radial points having surface densities of 8 up to 2048 $M_\odot$ pc^{-2} are also plotted.

an exponential function:

$$\tau_{sf} = 12.6 \exp\left[-0.53M\right] \qquad (3.7)$$

where M is the size of the offset in magnitudes. Since, in our model, the isochrone is a direct measure of the degree to which astration has consumed the available gas supply, the relationship found in Paper I between the offset parameter and the mean surface density of gas (and the Hubble type of the galaxy) has a natural physical explanation. In Figure 5 we give the relationship between mean surface density of H I and τ_{sf} using the values drawn from Table 2. The line is the linear least-squares fit. This confirms the connection between star formation age and remaining gas supply.

4. PHYSICAL MODELS FOR STAR FORMATION

The existence of a relationship, universal to all disk galaxies, coupling star formation with the total surface density and the surface density of gas, is a strong indication that the rate of star formation is controlled locally within a disk, rather than depending more generally on galaxian environment. This viewpoint obtains additional support through the fact that the global rate of star formation does not appear to be seriously affected by, for example, the spiral density waves, which seem to organize the star formation into certain regions of the galaxy, rather than influencing the total rate (Paper I). In the previous section, we have established the range of Schmidt Law indices which are consistent with the observational

material. In this section we investigate the physics of star formation processes in greater detail to discover what kind of Schmidt Laws might be expected on different scenarios, and hence which of these (if any) seem to be favored by the observational material.
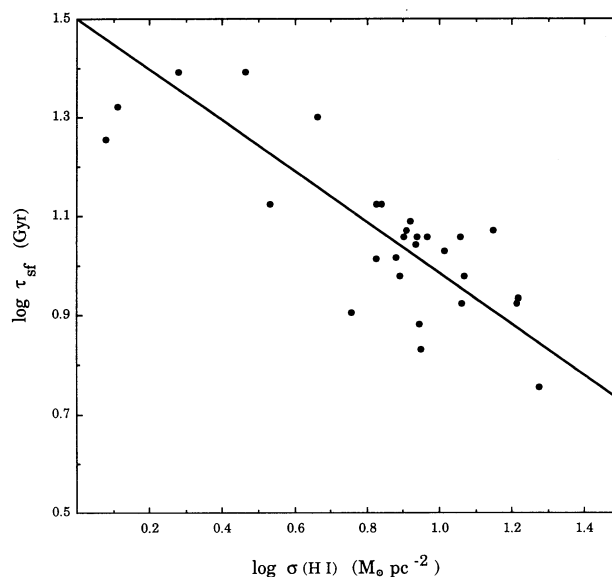

FIG. 5.—Estimated mean star formation age defined in the text compared with the mean H I surface density for the galaxies listed in Table 2.

TABLE 2

PARAMETERS OF THE SURVEY GALAXIES

Galaxy (1)	$R_0(I)$ (kpc) (2)	σ (H I) ($M_\odot$ pc^{-2}) (3)	τ_{sf} (Gyr) (4)	R_{10} (kpc) (5)	Ω_{10} (km s^{-1} kpc^{-1}) (6)	$L_{H\alpha}(R_{10})$ ($L_\odot$ pc^{-2}) (7)
NGC 45	2.17	11.4	11.4	...	...	...
NGC 1187	2.89	6.7	10.3	8.8	47	0.275
NGC 1313	1.09	18.8	5.7	3.5	87	0.509
NGC 1398	4.04	3.5	8–19	14.5	47	0.127
NGC 1637	1.48	14.1	11.8	4.1	71	0.109
NGC 1640	1.72	16.4	8.4	6.1	...	0.371
NGC 1688	1.47	11.7	8–11	4.3	53	0.216
NGC 1744	1.83	8.0	11.4	3.3	71	0.233
NGC 1808	2.51	4.8	11–23	5.0	65	0.127
NGC 2217	4.58	4.6	15–23	13.7	56	0.110
NGC 2427	3.07	6.7	13.3	7.2	40	0.232
NGC 2442	3.59	7.5	6–11	11.8	51	0.289
NGC 2835	2.81	8.9	6.8	7.8	34	0.661
NGC 2997	5.09	6.9	13.3	15.4	24	0.130
NGC 3059	1.99	11.5	8.4	7.0	56	...
NGC 3115	1.74	1.9	24.7	6.7	42	0.044
NGC 3175	2.25	...	...	4.6	...	0.017
NGC 3351	2.09	3.4	13.3	7.1	55	0.147
NGC 3368	2.16	4.6	19.9	8.0	60	0.069
NGC 3423	1.88	8.7	11.4	5.2	62	...
NGC 3593	0.90	1.3	20.9	2.9	87	0.068
NGC 3621	1.97	16.5	8.6	7.3	42	0.247
NGC 4192	5.75	2.9	24.7	12.3	39	...
NGC 4548	3.79	1.2	18.0	13.1	32	0.177
NGC 5068	1.88	8.8	7.6	5.9	39	0.446
NGC 5643	2.77	7.6	10.4	12.0	44	0.177
NGC 6118	4.16	4.2	6, 11, 15	13.8	27	0.182
NGC 6384	5.82	5.7	6.6, 9.5	19.8	27	0.495
NGC 6744	4.99	8.3	12.3	15.9	29	0.156
NGC 7205	2.26	8.6	11.0	9.6	56	0.170
NGC 7424	4.99	10.3	8.4, 13	10.1	35	0.433
IC 4710	1.48	7.8	9.5	3.9	27	0.273
IC 5201	5.26	8.1	11.8	5.5	44	0.138
IC 5332	2.40	9.3	11.4	5.4	40	0.166

4.1. Global Gravitational Instabilities in the Disk

There are a number of well-known mechanisms whereby gravitational instabilities in a thin, rotating, gravitationally unstable gas layer can lead to star formation. The key parameter which measures the gravitational instability in a layer with surface density σ_g and with a mean velocity dispersion $\langle v_g \rangle$ is the Toomre parameter, Q (Toomre 1964):

$$Q = \kappa \langle v_g \rangle / \pi G \sigma_g , \qquad (4.1)$$

where κ is the local epicyclic frequency. In galaxies with a flat rotation curve, the epicyclic frequency is directly related to the angular velocity, Ω, by $\kappa = 2\Omega$. The criterion for gravitational instability is $Q < 1$. However, instabilities may still occur for $Q > 1$ if magnetic fields can exercise large-scale control of gas motions (Elmegreen 1987), or if the differential motions allow "swing-amplification" to occur. These are important in the range $1 < Q < 2$ (Toomre 1981; Larson 1984). The characteristic growth time of the gravitational instability is given by

$$\tau_{grav} = \langle v_g \rangle / \pi G \sigma_g \qquad (4.2)$$

if the velocity dispersion of the gas layer is the same everywhere in the disk, which appears to be the case to a first approximation. Assuming that the timescale for star formation is governed by this timescale, then the star formation rate per unit area in the disk is given by (Larson 1988)

$$d\sigma_* / dt = \beta \sigma_g / \tau_{grav} \propto \sigma_g^2 . \qquad (4.3)$$

This recovers the "classical" Schmidt Law, and is the physical justification for it.

Numerical simulations of the swing-amplification process in galactic disks by Sellwood & Carlberg (1984) and Carlberg & Freedman (1985) show rather that the stability parameter Q tends to self-regulate near the upper bound of instability, $Q \sim 2$. In this case the velocity dispersion is no longer constant, and equation (4.2) should be replaced by

$$\tau_{grav} = Q/\kappa , \qquad (4.4)$$

leading to

$$d\sigma_* / dt \propto \Omega \sigma_g \qquad (4.5)$$

(Larson 1988; Silk 1988; Wyse & Silk 1989).

The results of § 3 do not exclude equation (4.3) as a possibility, nor do we have the rotation curves which would allow us to test how well equation (4.5) works. Indeed, Larson (1988) has pointed out that in galaxies with a flat rotation curve, Ω scales roughly as $1/R$, and since Ω is high in regions nearer the center where σ_g is also high, star formation of the form (4.5) would be hard to distinguish from that of equation (4.3).

In order to perform a more quantitative test, we have taken for each of the galaxies the Hα luminosity at the point, R_{10}, where the surface brightness in the I-band is 10 $L_\odot$ pc^{-2}. This is given in column (7) of Table 2. The radius R_{10}, given in column (5) of Table 2, is sufficiently far out in each galaxy compared with the scale length (col. [2]) that we can assume

that the rotational velocity has reached its maximum value. We have estimated this from the Reif et al. (1982) W_{20}-values, correcting for inclination effects using the values obtained in Paper I. The angular velocity Ω_{10} that this implies at R_{10} is given in column (6) of Table 2.

We compare the star formation rate at R_{10} with the *mean* surface density in H I, σ(H I) in Figure 6a, and with the product of the angular velocity and surface density in Figure 6b. The main uncertainty here is the question of how well the mean H I surface density is representative of, or scales with, the actual surface density at R_{10}. We will not be able to resolve this until we have H I maps for many more of these galaxies. Nonetheless, surveys such as that of Wevers (1984) allow some optimism that this is the case.

In Figure 6a, there is a clear correlation between surface density and star formation rate. This is of similar quality to the correlation between the *global* star formation rate and the total H I mass found in Paper I. However, the least-squares fit to this correlation gives a slope of 1.1 ± 0.5, which is inconsistent with the "classical" Schmidt Law form given by equation (4.3). The problem with this result is that a slope as shallow as this is ruled out on the basis of the observational results of the previous section. However, this problem would be avoided if there is also a dependence on total surface density, since this parameter has been eliminated in Figure 6a by the choice of a reference surface density for all galaxies.

Even neglecting any possible dependence of star formation rate on total surface density, Figure 6a is probably insufficient evidence to rule out a power law with a higher index on the gas surface density, since the molecular component is not included.
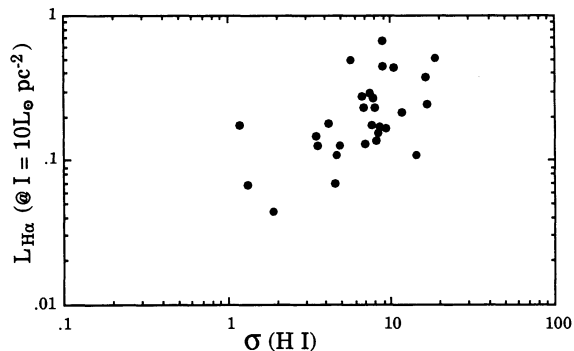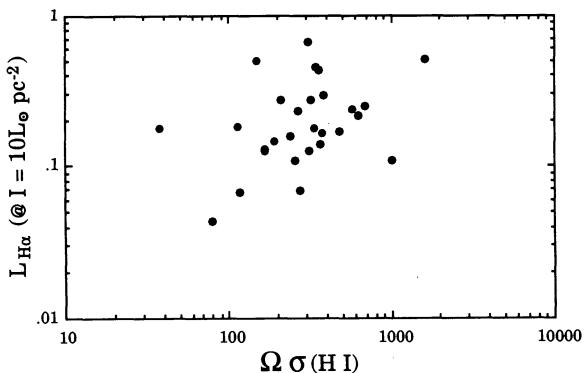

FIG. 6a

FIG. 6b

FIG. 6.—Correlation between the Hα luminosity at the point where the *I*-band luminosity is 10 $L_\odot$ pc^{-2} and (a) the mean surface density in H I, and (b) the product of the H I surface density and the angular velocity at this same point.

In other, more detailed observational studies, the evidence is conflicting. For example, in M31 and M33, the observations appear to follow a "classical" Schmidt Law in cells of ∼500 pc across (Nakai & Sofue 1982; Freedman 1986). The Donas et al. (1987) sample likewise is consistent with a higher index. However, Young (1988a) finds a higher power law index in the spiral arms of M51 than in the interarm region.

Figure 6b shows effectively no correlation (the correlation coefficient is less than 0.1), and this seems to militate strongly against swing-amplified self-regulating star formation. However, the definitive answer to this question will have to wait until H I surface density profiles and rotation curves are available for more of these galaxies.

4.2. *Gravitational Instability in Molecular Clouds*

The rate of star formation cannot be entirely controlled by the rate of growth of gravitational instabilities within individual molecular clouds. It has long been recognized that the lifetime of molecular clouds is at least an order of magnitude longer than their free-fall timescales (Kwan 1979; Blitz & Shu 1980) and the typical turbulent velocities are highly supersonic. It is clear that an energy source is needed to give the required turbulent support. Norman & Silk (1980) and Franco (1983) suggested that the winds from young stellar objects might provide this energetic input. Franco & Cox (1983) were able to derive a stellar birthrate on the assumption that this turbulent input also serves to regulate the rate of low-mass star formation within molecular clouds (see also the review by Falgarone & Puget 1988). By this model, the rate of star formation per unit mass is given by (to a first approximation):

$$(1/M_c)dM_*/dt = cf_m n_3^{5/8} , \qquad (4.6)$$

where f_m is the fractional volume filled with matter, and n_3 is the particle density of the cloud in units of 10^3 cm^{-3}. To the degree that the ensemble average $\langle f_m n_3^{5/8}\rangle$ is constant, equation (4.6) implies a Schmidt Law of the form $d\sigma_*/dt \propto \sigma_g$.

There exists direct observational evidence (Fukui et al. 1986; Lada 1988) that the energy input from the CO outflow sources is sufficient to balance the molecular clouds against turbulent dissipation, provided that the timescale over which this operates is an order of magnitude greater than the free-fall timescale. Furthermore, the observed mass:radius or velocity dispersion:radius relations also support this picture. Larson (1981) found from observation that cloud mass M_c, radius R_c, and velocity dispersion Δv, are related through $M_c \propto R_c^2$ and $\Delta v \propto R_c^{1/2}$. Chièze (1987) has shown that this is exactly what would be expected if the interstellar clouds are close to gravitational instability in a constant pressure environment, and suggests that the subcondensations may form a gravitational *N*-body system in a quasi-static virialized condition, leaving the scaling relationships unchanged for the individual fragments. In this case the following relationships apply

$$M_c/M_\odot = 142(P/3800 \text{ K cm}^{-3})^{1/2}(R_c/\text{pc})^2 \qquad (4.7)$$

and

$$(\Delta v/\text{km s}^{-1}) = 0.68(P/3800 \text{ K cm}^{-3})^{1/4}(R_c/\text{pc})^{1/2} , \qquad (4.8)$$

where P is the stochastic mean pressure in the ISM. It is interesting to note that the surface density implied by equation (4.7) is just a little greater than the critical surface density required for clouds to survive collisions with external diffuse material to accrete matter in such a collision, rather than being ablated

away. Larson (1988) shows that the condition for survival is that the gravitational binding pressure should exceed the ram pressure tending to disrupt the cloud: $G\sigma_c^2 > \rho\langle v\rangle^2$, where σ_c is the surface density of the cloud and $\langle v\rangle$ is the characteristic velocity of the collision. A diffuse cloud at $T \sim 200$ K in pressure equilibrium with the other phases of the disk medium will have a density of about 18 cm^{-3} and, for a typical velocity dispersion of 10 km s^{-1}, the critical cloud surface density required for survival will then be $\sim 100\ M_\odot$ pc^{-2}, compared with the 140 $M_\odot$ pc^{-2} implied by equation (4.7).

In what follows, we assume that molecular clouds lie in virial equilibrium on the curves given by equations (4.7) and (4.8), and that these clouds grow by cloud-cloud accretion and coalescence. Such clouds will be destroyed by occasional high-velocity collisions or by the energetic input of the young, massive stars (stellar winds, ionizing radiation and supernova explosions). These clouds also have a low-mass star formation rate which is just sufficient to keep them on the brink of catastrophic gravitational collapse.

On this model, the rate of star formation in individual molecular clouds can be estimated by consideration of their CO luminosity. Molecular clouds in galaxies dissipate their internal turbulence by shocks, which radiate predominantly in CO lines at solar abundances and at the densities which are typical for these clouds. Thus, the CO emission is a direct indicator of the rate of energy dissipation within molecular clouds, and probably tells us little about the total molecular content, especially of molecular hydrogen. This then gives a natural explanation for the very tight one-to-one correlation of CO luminosity and star-formation activity found in metal-rich galaxies such as M51 and NGC 6946 (Young 1988a), since the rate of mechanical energy dissipation is very closely related to the star formation rate. For a cloud which is optically thick in ^{12}CO, the CO lines emit at the blackbody emissivity, and so the luminosity, L_{CO}, can be written (Young 1988b) in terms of the radius of the molecular cloud R_c, the line width Δv, and the cloud temperature T_C:

$$L_{CO} = \pi R_c^2\, \Delta v T_C .\qquad (4.9)$$

Substituting equations (4.7) and (4.8) for the cloud radius and velocity dispersion into equation (4.9) we have

$$L_{CO} \propto T_C\, M_c^{5/4} .\qquad (4.10)$$

To the extent that all molecular clouds can be considered to be at the same temperature, this agrees to high precision with the observational correlation between CO luminosity and mass for individual molecular clouds in our Galaxy (Solomon et al. 1987). This is shown in Figure 7 for clouds in our solar neighborhood. At low abundance, presumably the main cooling mechanism of the clouds would be through molecular hydrogen line emission rather than through ^{12}CO line cooling. However, since equation (4.9) applies to any optically thick line emission, the same scaling relationship between mass and line luminosity should apply, but with a different constant of proportionality.

For collisional growth of clouds moving with mean velocity $\langle v\rangle$ in an intercloud medium of density ρ, the cloud mass increases exponentially with a characteristic growth time $\tau = \sigma_c/\rho\langle v\rangle \sim 10^8$ years. In the case that cloud growth is limited by cloud coagulation rather than collisional fragmentation, the mass spectrum is a power-law mass distribution having $n(M) \propto M^{3/2}$ up to a maximum mass M_{max} above which it cuts off sharply, presumably due to cloud destruction by massive
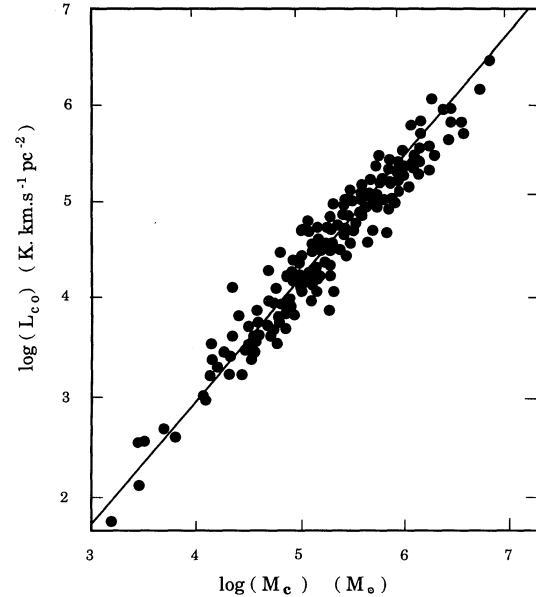

FIG. 7.—Virial mass vs. CO luminosity relationship observed for individual molecular clouds in the Galaxy by Solomon et al. (1987), compared with a line having the theoretical slope of 5/4 as derived in the text.

star formation (Field & Saslaw 1965; Penston et al. 1969; Tomisaka 1984, 1986). The theoretical mass distribution is in good agreement with observations (Sanders, Scoville, & Solomon 1985). In this case, equation (4.10) implies that the specific rate of star formation will scale as $M_{max}^{1/4}$. Once again, to the degree to which M_{max} is a constant, this implies a Schmidt Law of the form $d\sigma_*/dt \propto \sigma_g$.

In conclusion, star formation resulting from gravitational instabilities within individual clouds results in an approximately constant specific rate of star formation (per unit mass). This result may well apply for the proportion of the low-mass star formation which occurs continually in galactic disks, and provides the turbulent support of the molecular clouds, but it cannot be true for the majority of intermediate- and high-mass star formation, since Schmidt Laws of the form $d\sigma_*/dt \propto \sigma_g$ are definitely excluded on the basis of the results of the previous section. Clearly a more complex model of star formation in galactic disks is required.

4.3. Self-Regulation in Galactic Disks

The models described in the earlier sections deal only with gravitational instabilities within disks or individual molecular clouds. However, this is unlikely to represent the whole story, since the energy and momentum input from massive stars must also have some effect. We know, for example, that the energy input of massive stars exercises fundamental control on the phase properties and the mean pressure of the ISM. This is the basis of the multi-phase models (Field, Goldsmith, & Habing 1969; Cox & Smith 1974; McKee & Ostriker 1977; Cox 1979, 1980), although these differ in emphasis, and in the details of how such a multi-phase medium is set up and maintained. It is likely that the energy input of massive stars also exercises some control on the local rate of star formation through negative feedback processes. As a practical example of how such a feedback can occur, consider a giant localized burst of star formation in the plane of the disk. In this case, energy input from stellar winds and supernova explosions will give rise first to an

expanding bubble (as seen, for example, in NGC 1313; Ryder et al. 1994). If the bubble breaches the gas disk, it will cause a (one- or two-sided) galactic "chimney" to be formed (Bregman 1980; Tomisaka & Ikeuchi 1986; McCray 1988), blasting disk gas to large heights, and ensuring that a "refractory" period will follow in which star formation is locally suppressed until the hole in the ISM has filled up again. These ideas represent the basis of the stochastic self-propagating model of star formation (Feitzinger & Braunsfurth 1984; Spicker & Feitzinger 1988a, b). Struck-Marcell & Scalo (1987) have considered in detail the chaotic limit cycle behavior that occurs where starbursting behavior is dominant. In some situations the cloud-cloud collision timescale need no longer be a simple monotonic function. However, these models did obey a classical Schmidt Law as long as the star formation rate remained below a burst threshold. In the burst case there is a large scatter around the Schmidt Law relation. In this paper we will be considering rather a quiescent, self-regulating disk. In this case "bursts" are assumed to occur locally on too short a timescale to affect the global properties of the disk.

Dopita (1985) argued that these energetic processes also stir up the ISM to maintain the vertical w-velocity dispersion in disk galaxies. By assuming an equipartition between turbulent and thermal pressures in the disk medium, he derived a model for the rate of formation of massive stars having a Schmidt Law with indices $n = 1$; $m = 1$. As has been shown in the previous section, this is not in particularly good agreement with observations. Here we abandon the (somewhat arbitrary) equipartition assumption, and consider instead a model in which star formation is moderated by cloud-cloud collisions. This type of model is more satisfactory from a philosophical viewpoint in that it invokes a known physical process for star formation; namely, the development of large-scale gravitational instabilities in either the shocked layer between two clouds (Mouschovias, Shu, & Woodward 1974; Elmegreen 1979, 1982; Cowie 1981; Balbus & Cowie 1985), or within individual molecular clouds as described in § 4.2. The assumption that the star formation rate is proportional to the cloud-cloud collision timescale τ_{cc}, gives (cf. eq. [4.3]):

$$d\sigma_*/dt = \beta \sigma_g/\tau_{cc} , \qquad (4.11)$$

where β is a constant of proportionality. An equation of the form of (4.11) will also apply in an aggregation model of star formation in clouds which grow until the process is terminated by the formation of massive stars in the most massive molecular clouds, which in turn destroys them. The reason why equation (4.11) can give rise to a Schmidt Law which has a different index to that of equation (4.3) is that the cloud-cloud collision timescale is now moderated by physical conditions in the local galaxian environment.

Cloud-cloud collisions occur at low velocities, and therefore undergo radiative losses. However, they do conserve momentum, and as a consequence tend to reduce the velocity dispersion of the gas in the vertical (w-) plane. Many of the energetic processes associated with the high-mass mode of star formation, such as mass-loss driven bubbles or supernova shells, are also radiative and momentum-conserving in their late evolutionary stages. However, these serve to balance the effect of cloud-cloud collisions by increasing the velocity dispersion of the gas in the $+w$ and $-w$ directions. In effect, we can regard these processes as being responsible for the high-latitude H I "cirrus," the H I Lockman Layer (Lockman 1984) and the warm ionized Reynolds Layer in our Galaxy (Reynolds 1991,

1992). In the steady state we expect a momentum balance:

$$\kappa v_{ej}(d\sigma_*/dt) = \sigma_g v_g/\tau_{cc} , \qquad (4.12)$$

where v_g is the vertical w-velocity dispersion of the cloudy gaseous layer with surface density σ_g and characteristic cloud-cloud collision timescale τ_{cc}, v_{ej} is a characteristic velocity of ejection of matter from massive stars, and κ is a coupling constant between the mass ejected from the high-mass stars, and the mass swept up by winds, supernovae, etc. To the extent that the IMF and the energy yield from the high-mass stellar population does not depend on metallicity, κ and v_{ej} are independent of galaxian environment.

Equations (4.11) and (4.12) together imply that

$$v_g = \beta \kappa v_{ej} . \qquad (4.13)$$

That is to say, the vertical velocity dispersion of the gas in *all disk galaxies* should be the same, and independent of the radial coordinate. This is an observed property of all disk galaxies, covering a wide variety of morphological type, which have so far been observed (van der Kruit & Shostak 1984, and references therein; Meatheringham et al. 1988; Stark & Brand 1989). The H I velocity dispersion is observed to be of order $6-10$ km s^{-1}, and shows little variation between the arm and interarm regions. However, it is seen to locally increase in regions of active star formation, such as the 30 Doradus region in the LMC. This is entirely consistent with our hypothesis.

Massive star formation provides the background pressure of the ISM in the plane of disk galaxies. Furthermore, because the hot gas from supernova explosions can bubble up to form a hot halo to the galaxy (Chevalier & Oegerle 1979; Bregman 1980; Tomisaka & Ikeuchi 1986; McCray 1988), the scale height for pressure variation is large compared with the matter scale height, and the cooling timescale of this phase can be long compared with the lifetime of individual OB stars. For a solar composition plasma at $\sim 10^6$ K cooling isobarically in a non-equilibrium fashion, a fit to the Sutherland & Dopita (1993) cooling functions gives:

$$\tau_{cool} = 4.5 \times 10^7 \; T_6/n_{-3} \; \text{years} , \qquad (4.14)$$

where T_6 is the electron temperature in units of 10^6 K, and n_{-3} is the particle density in units of 10^{-3} cm^{-3}. Since the sound speed of a plasma at 10^6 K is 123 km s^{-1}, the gas pressure can be communicated over a distance of ~ 10 kpc within a cooling timescale. As Chevalier & Oegerle (1979) have shown, there exists a critical temperature T_{crit} for the hot coronal halo, above which a galactic wind is generated:

$$T_{crit} = \frac{\gamma - 1}{\gamma} \frac{\mu m_H}{k} \left\{ \frac{v_{esc}^2}{2} - \frac{v_{rot}^2}{2} \right\} , \qquad (4.15)$$

where v_{esc} is the escape velocity at the radial point R in the galaxy considered, and v_{rot} is the rotational velocity of the disk at this same point. For a galaxy with a flat rotation curve out to some critical radius R_{out}, outside of which the halo mass density falls to zero,

$$v_{esc}^2 = 2v_{rot}^2\{1 - \ln[r/R_{out}]\} . \qquad (4.16)$$

It is reasonable to assume that in real galaxies, the temperature is kept near the critical temperature given by equation (4.15), since in our own Galaxy at least, the scale height of the hot phase ($\sim 2-3$ kpc) is appreciably larger than all other scale heights (Pettini & West 1982; Savage & Massa 1985, 1987). Temperatures much lower than this would allow the hot halo

gas to cool, and temperatures much higher than this would cause the halo gas to be lost in a wind. To maintain a galactic fountain flow in stochastic equilibrium, the cooling timescale for the hot phase would have to be matched to the timescale for its replenishment, i.e., the timescale for star formation. From our basic assumption (eq. [4.11]), this timescale is given by the cloud-cloud collision timescale τ_{cc}. Therefore, from taking the critical temperature given by equation (4.15), we can rewrite the cooling timescale (4.14) in terms of the local escape velocity and stochastic mean pressure in the ISM:

$$\tau_{cool} = \tau_{cc} = \alpha v_{esc}^2/P , \qquad (4.17)$$

where α is some constant of proportionality.

In order to explicitly derive a star formation rate from these equations, we must recall that the cloud-cloud collision timescale depends not only on the local pressure, but also on the motion of the gas clouds in the potential determined by not only these gas clouds, but also by the stellar component. In the van der Kruit & Searle (1981a, b; 1982) disk model, the solution to the Poisson equation gives a z-density distribution of matter $\rho(z) = \rho(0) \, \text{sech}^2 \, (z/z_*)$. This function tends to an exponential for $z > z_*$. The total matter surface density σ_T is related to the mid-plane velocity dispersion of the stars, v_*, by

$$v_*^2 = \pi G \sigma_T z_* . \qquad (4.18)$$

The gas velocity dispersion is considerably less than v_* generally; therefore the gaseous scale height is also less. In the case that the disk matter distribution is exponential, and the gas can be regarded as a subpopulation in the same potential, but with different scale height, the mid-plane velocity dispersion is given (exactly) by

$$v_g^2 = 2\pi G \sigma_T z_g^2/(z_* + z_g) , \qquad (4.19)$$

where the scale heights are now defined in terms of the scale heights of the exponential, half that of the previous definition. The one-dimensional velocity dispersion of the giant molecular clouds (GMCs) in our solar neighborhood has been measured by Stark & Brand (1989) at 8 km s^{-1} (rms). This is the same as the vertical velocity dispersion of the LMC GMCs (Cohen et al. 1988), and similar to the H I vertical velocity dispersions measured in other galaxies, as would be expected if the velocity ellipsoid is isotropic.

To solve this set of equations in terms of the total star-formation rate, we require an explicit expression for the cloud-cloud collision timescale, τ_{cc}. This can be written in terms of the scale height of the gas, the velocity dispersion of the gas, and the area covering factor of molecular clouds in the gaseous disk, f, as

$$\tau_{cc} = 2z_g/v_g f . \qquad (4.20)$$

However, we know from § 4.2 that the clouds act as if they are in marginal equilibrium against collapse with the external pressure, and that they therefore obey the scaling relationships (4.7) and (4.8), which imply a constant effective surface density for all clouds at a given pressure. Thus the area covering factor, normalizing to some arbitrary point in the disk, is given by

$$f = f_0(P/P_0)^{-1/2}(\sigma_g/\sigma_0) , \qquad (4.21)$$

where P_0 and σ_0 are the reference pressure and surface density, respectively. Substituting equations (4.21), (4.20), (4.19), and (4.17) back into equation (4.11) and solving for the star formation rate yields

$$d\sigma_*/dt = \epsilon v_{esc}^{-2/3}(z_* + z_g)^{-1/3}\sigma_T^{1/3}\sigma_g^{5/3} , \qquad (4.22)$$

where all the constants and normalization factors in the scaling relationships have been subsumed into a single constant ϵ, which can be regarded as an efficiency factor for star formation. The power-law indices of the various parameters in equation (4.22) can be qualitatively understood in terms of their effect on the cloud-cloud collision timescale. Clearly, gas-rich systems will have shorter cloud-cloud collision timescales than gas-poor systems. A high mass surface density will work toward shorter cloud-cloud timescale. Clearly, gas-rich systems will have shorter cloud-cloud collision timescales by reducing the scale heights. A deep potential will permit high intercloud pressures, tending to lengthen the cloud-cloud collision timescale.

As pointed out earlier, pressure disturbances can be communicated very quickly in the hot gas. The fact that the heating is local and impulsive, generating local pressure variations, argues for the importance of local hydrodynamic forces in affecting the self-regulation process. Expansion cooling is also likely to be important in local flows. In this sense, equation (4.22) represents the limiting case of perfectly self-regulating star formation in real disks. Clearly, a dynamical treatment incorporating the physical processes summarized here would represent the next major step forward in the development of these ideas.

Equation (4.22) has some very interesting consequences. Although it basically takes the form of a Schmidt Law with indices $n = 1/3$; $m = 5/3$, these indices are further modified by the local scale heights and the depth of the potential. For example, in galactic bulge regions where both z_* and v_{esc} are large, we would expect star formation rates to be depressed. Equation (4.16) shows that the escape velocity changes slowly with radius, and in any case, in the star-forming disk of a galaxy with a flat rotation curve, $r \ll R_{out}$, usually. We can therefore assume that v_{esc} scales as v_{rot} for most galaxies. The implication is that large galaxies are somewhat less efficient at forming stars at a given surface density, thanks to the higher halo pressure which reduces the cloud collisional timescales.

As far as scale heights are concerned, it must be recalled that these are dependent both on the surface density of the disk, and on the age of the disk. From equations (4.13) and (4.19), and provided that the stellar scale height remains constant with radius (van der Kruit & Searle 1981a, b, 1982) and appreciably larger than the gas scale height, we have $z_g \propto \sigma_T^{-1/2}$ in the gaseous layer. Thus the gas layer in an exponential disk with $\sigma_T(r) = \sigma_0 \exp \, [-r/R_0]$ will have $z_g(r) = z_0 \exp \, [+r/2R_0]$. This flaring of the gas disk is consistent with the observations of the H I and the molecular layers in our Galaxy (Downes & Güsten 1982; Sanders et al. 1984; Grabelsky et al. 1987).

A classic problem in stellar dynamics is that the velocity dispersion and scale height of stars appear to increase with age (Wielen 1977; Twarog 1980; Wielen & Fuchs 1983). A likely explanation for the scale height:velocity dispersion:age relationships observed in our solar neighborhood is that the velocity dispersion is increased with time by stellar orbital diffusion caused by gravitational scattering by giant molecular clouds. Such an evolution was originally proposed by Spitzer & Schwarzschild (1951, 1953), and the idea has been further developed by Wielen (1977), Vader & de Jong (1981), Lacey (1984), and Villumsen (1985). According to this theory, stars are born with some initial velocity dispersion $v_*(0)$, which we can take to be the same as the velocity dispersion in the gaseous thin disk. At time t, they will have acquired a velocity dispersion $v_*(t)$ given by

$$v_*(t) = v_*(0)[1 + t/t_{diff}]^{1/3} . \qquad (4.23)$$

This equation remains valid only for so long as the scattering clouds and the stars can be considered to remain in the same layer. The breakdown of this assumption leads to a change in the exponent. Wielen (1977) finds empirically that an exponent of $\frac{1}{2}$ gives a good fit to the observations, whereas both Lacey (1984) and Villumsen (1985) find that a rather lower exponent in the range 0.25–0.35 is a better fit to the theoretical models. The diffusion or scattering timescale, t_{diff}, depends on the characteristic mass M_c, and space density n_c, of the scattering centers. The Spitzer-Schwarzschild formulation gives

$$t_{\mathrm{diff}} = 4v_*(0)^3/(3\pi^{3/2}G^2M_c^2 n_c \ln[a]) , \qquad (4.24)$$

where a is an impact parameter. From this equation, we can infer that locally in our Galaxy, t_{diff} is of order 5×10^7–1.5×10^8 years. From equation (4.18), we see that equation (4.24) implies $t_{\mathrm{diff}} \propto \sigma_T^{3/2}z_*^{3/2}\sigma_g^{-1}z_g$. In the limit of a young gas-rich galactic disk, $t_{\mathrm{diff}} \propto \sigma_T^{-1/2}$ so diffusion proceeds more rapidly in regions of high surface density. At late times on the other hand, $t_{\mathrm{diff}} \propto (\sigma_T/\sigma_g)z_*^{3/2}$, so the diffusion time is driven more by the gas fraction.

Using these diffusion equations and the star formation model given in equation (4.22), we have constructed a model for the solar neighborhood. We have assumed an infall timescale of 2.5 Gyr, a surface density of 67 $M_\odot$ pc^{-2}, and a local velocity of escape of 500 km s^{-1}, near the mid-range of the estimates given in the review by Fich & Tremaine (1991). Again, we adjusted the star formation efficiency to give 13.5 $M_\odot$ pc^{-2} of gas remaining after 13 Gyr of evolution. The stellar diffusion timescale was adjusted so as to yield the observed scale heights of the molecular layer (80–100 pc) and the local stellar disk (290–330 pc) at the current epoch. This requires $t_{\mathrm{diff}} = 1.25 \times 10^8$ yr, in good agreement with other estimates of this quantity. The exponent of the velocity diffusion law (eq. [4.23]) was taken as 0.25 to allow for diffusion of the stars out of the scattering layer. The results are shown in Figure 8. Note that the stellar and gaseous scale heights are initially large as a result of the low surface density in the disk (ram pressure confinement is not taken into account in this simulation). The disk scale heights reach a minimum near the peak of the gas surface density, and then increase as a result of dynamical heating of the stars and the decrease in the gas surface density. The peak of the star-formation activity occurs a little later than in the simple Schmidt Law model of Figure 2.

Some of the physics that has gone into deriving equation (4.22) has only been considered previously by Talbot & Arnett (1975). Their Standard Flattened Exponential Galaxy model starts with an exponential radial mass profile, and incorporates the surface mass density in the prescription for star formation, through its influence on the gas pressure in the plane and on the vertical velocity dispersions of the gas and the stars. They considered both a simple power-law parameterization of the star formation rate, as well as a metallicity-enhanced version. Their $\kappa = 3/2$ power law is analogous to our $n = 0.5$; $m = 1.5$ model in equation (3.1), and in fact gives the closest match to our Figure 1 out of all of their models. They too argued for a critical gas temperature on the basis that increased gas turbulent motions result in enhanced dissipation and more efficient cooling. Most of the differences in our findings result from improvements in the observational constraints, molecular cloud physics, and treatment of the evolution of the velocity dispersions.

In order to determine how well equation (4.22) can simulate the Hα surface luminosity versus stellar surface density relationship, we constructed two model galaxies having escape
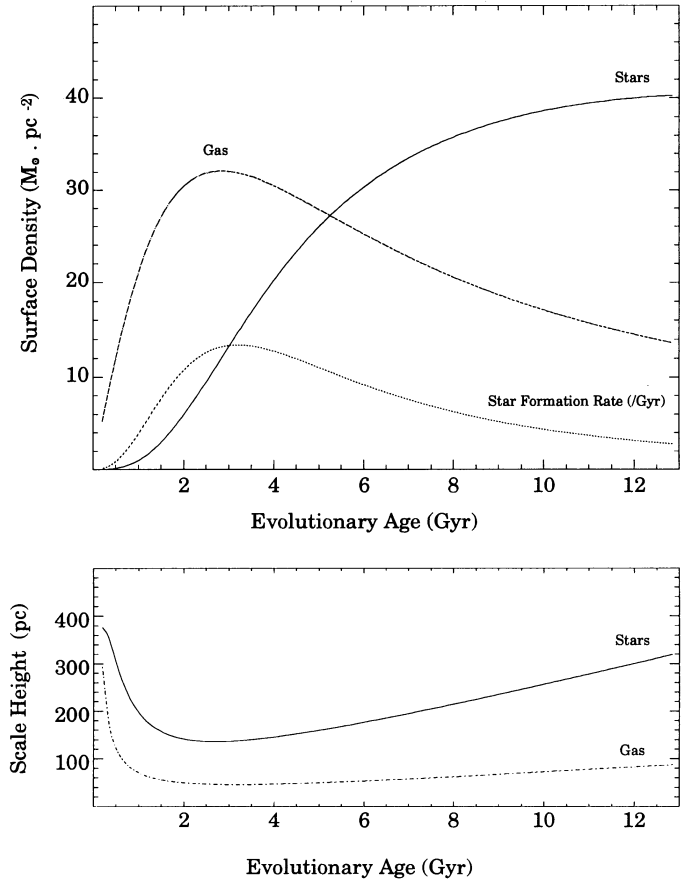

FIG. 8.—Evolution of the solar neighborhood according to the self-regulating star formation model described in the text.

velocities of 500 and 200 km s^{-1}, respectively, measured at a surface density of 64 $M_\odot$ pc^{-2}. The parameter R_{out} in equation (4.16) was taken to be 10 disk scale lengths to ensure a flat rotation curve out into the portion of the disk that is essentially gaseous, and a surface density of 2048 $M_\odot$ pc^{-2} was assumed to occur at 1 disk scale length from the center of the galaxy. The infall timescale was assumed to scale as $1/v_{\mathrm{esc}}$. This allows the collapse of low-mass galaxies to occur over a longer time frame. The results of this simulation are given in Figures 9a and 9b. The agreement with the observed slope is excellent, and it is clear that at least some of the scatter in this relationship from galaxy to galaxy can be ascribed simply to differences in infall timescale resulting from mass differences. The balance of the scatter may well be due to intrinsic age differences between galactic disks.

In Figure 10, we have plotted the computed radial structure of the model having an assumed exponential mass profile with escape velocity 500 km s^{-1} at a surface density of 64 $M_\odot$ pc^{-2}. This shows many of the characteristics of real galaxies, such as those observed by Wevers (1984). In particular, note how the exponential disk of stars steepens considerably at a surface density of ~ 10 $M_\odot$ pc^{-2} (or ~ 2.4 $L_\odot$ pc^{-2}). The gas disk follows the exponent of the mass distribution of the disk in the outer parts, but flattens at an equivalent H I content of about 4 $M_\odot$ pc^{-2}, remaining between 5 and 20 $M_\odot$ pc^{-2} of H I across the star-forming disk. Finally, the star formation rate in the disk has a scale length ~ 1.5 times longer than that of the older stars, in agreement with observations (Paper I). In this model
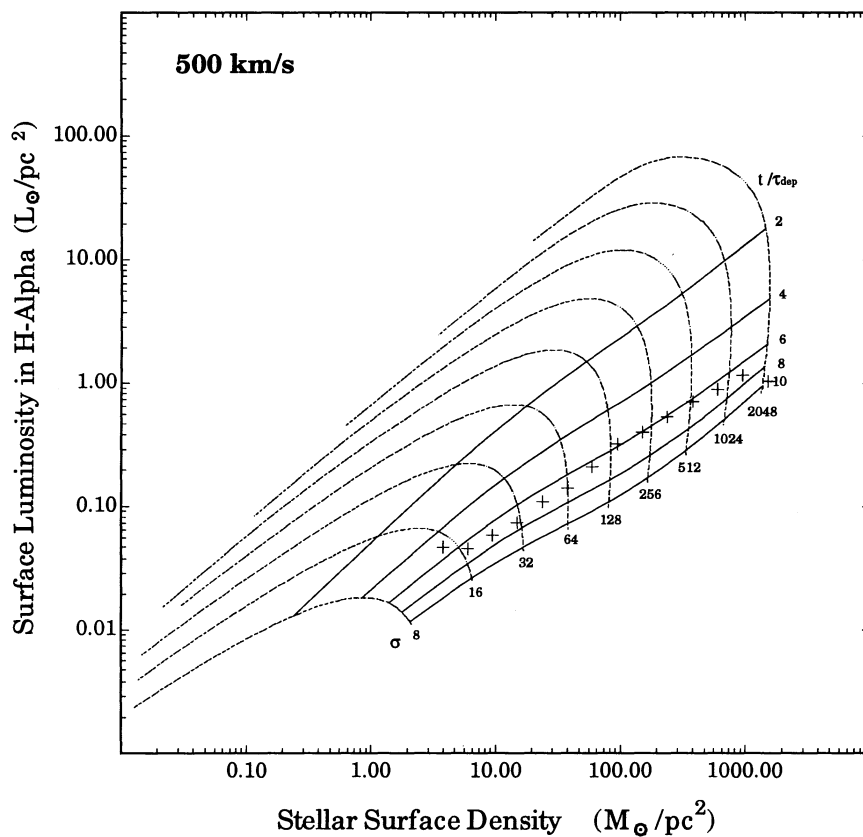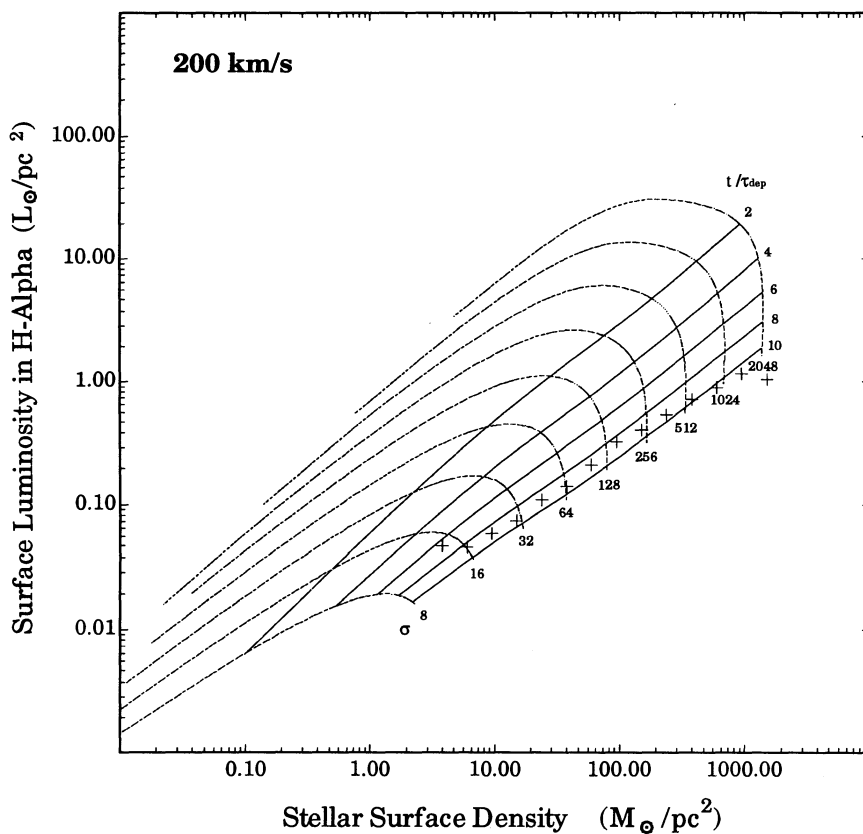
FIG. 9a

FIG. 9b

FIG. 9.—Full evolution of a model galactic disk having an escape velocity of (a) 500 km s^{-1}, and (b) 200 km s^{-1}, at a surface density of 64 $M_\odot$ pc^{-2}, according to the self-regulating star-formation model described in the text.
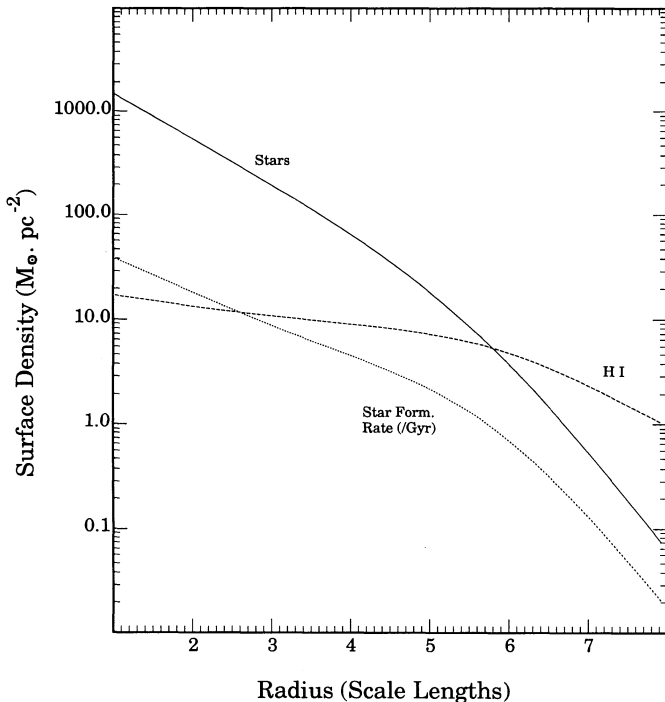
FIG. 10.—Inferred radial distribution of H I, luminous stars, and rate of star formation after 13 Gyr of evolution in the model disk galaxy described in the text. The final distribution of matter in the disk is assumed to follow an exponential law, and the observable H I content of the disk is obtained using the H I/(H I + H_2) conversion factor appropriate to the solar neighborhood given in § 3.3.

the H I to stellar ratio changes smoothly across the disk. In the simplest "closed-box" model for chemical enrichment, the chemical abundance of any primary nucleosynthetic element is given by (Searle & Sargent 1972): $Z(r) = Y \ln [\sigma_T/\sigma_g]$, where Y is the effective chemical yield of that element. Figure 10 then implies that the abundance gradient would have a scale length of ~ 2.2 times that of the underlying disk in the inner regions, but that this steepens in the outer parts to approach the same scale length as the disk.

In order to check these predictions, and to build more sophisticated models, it is clear that we require both the H I gas

profiles and the abundance gradients in the observational sample of galaxies. In addition, a measure of the true rotation curve will allow us to estimate the escape velocities, and to test for any effects resulting from radial flows. These data will be the subject of a future paper.

5. CONCLUSIONS

In this paper we have critically examined the various models of star formation in disk galaxies in the light of what we have learned from CCD surface photometry of a sample of nearby southern disk galaxies. The additional constraint furnished by these observations has allowed us to put new limits on the form of the law of star formation in disk galaxies. Assuming the rate of star formation to take a generalized Schmidt power-law form dependent on both the total local matter surface density, σ_T, and the gas surface density, σ_g; $d\sigma_*/dt = \epsilon \sigma_T^n \sigma_g^m$, we find that the observations constrain $(n + m) > 1$, and that the best fit is obtained from $1.5 < (n + m) < 2.5$. Both a Schmidt Law of the form $d\sigma_*/dt = \epsilon \sigma_g$, and a star formation law of the form $d\sigma_*/dt = \epsilon \Omega \sigma_g$, where Ω is the angular velocity at the radial point considered, seem to be excluded by observations. This result probably rules out models which depend on making stars quiescently in molecular clouds, and also rules out swing amplification star formation models.

We have suggested an alternative self-regulating star formation model which fits our observational material very well. The negative feedback in this model operates on the molecular clouds, by changing the cloud-cloud collision (or aggregation) timescales, and allows an understanding of the phase structure of the interstellar medium and the evolution of the vertical structure of the various components of galactic disks (stellar, molecular, atomic, and coronal). It is clear that a definitive test of these ideas must await a measurement of the rotation curve, the H I distribution, and the abundance gradients in these galaxies.

REFERENCES

Anders, E., & Grevesse, N. 1989, Geochim. Cosmochim. Acta, 53, 197
Arnett, W. A. 1978, ApJ, 219, 1008
Audouze, J., & Tinsley, B. M. 1977, ARA&A, 14, 43
Bahcall, J. N. 1984, ApJ, 276, 169
Balbus, S. A., & Cowie, L. L. 1985, ApJ, 277, 550
Belley, J., & Roy, J.-R. 1992, ApJS, 78, 61
Blitz, L., Fich, M., & Kulkarni, S. 1983, Science, 220, 1233
Blitz, L., & Shu, F. H. 1980, ApJ, 238, 148
Bosma, A. 1978, Ph.D. thesis, Univ. Groningen
———. 1981, AJ, 86, 1825
Bregman, J. N. 1980, ApJ, 236, 577
Buchhorn, M. 1992, Ph.D. thesis, Australian National Univ.
Burton, W. B., & Gordon, M. A. 1978, A&A, 63, 7
Carlberg, R. G., & Freedman, W. L. 1985, ApJ, 298, 486
Chevalier, R. A., & Oegerle, W. R. 1979, ApJ, 227, 398
Chièze, J.-P. 1987, A&A, 171, 225
Chiosi, C. 1980, ApJ, 83, 206
Chiosi, C., & Maeder, A. 1986, ARA&A, 24, 329
Cohen, R. S., Dame, T. M., Garay, G., Montani, J., Rubio, M., & Thaddeus, P. 1988, ApJ, 331, L95
Combes, F. 1991, ARA&A, 29, 195
Cowan, J. J., Thielemann, F.-K., & Truran, J. W. 1991, ARA&A, 29, 447
Cowie, L. L. 1981, ApJ, 245, 66

Cox, D. P. 1979, ApJ, 234, 863
———. 1980, ApJ, 245, 534
Cox, D. P., & Smith, B. W. 1974, ApJ, 189, L105
DeGioia-Eastwood, K., Grasdalen, G. L., Strom, S. E., & Strom, K. M. 1984, ApJ, 278, 564
de Vaucouleurs, G., de Vaucouleurs, A., Corwin, H. G., Buta, R. J., Paturel, G., & Fouqué, P. 1991, Third References Catalog of Bright Galaxies (New York: Springer)
Dickman, R. L., Snell, R. L., & Schloerb, F. P. 1986, ApJ, 309, 326
Donas, J., Deharveng, J. M., Laget, M., Milliard, B., & Huguenin, D. 1987, A&A, 180, 12
Dopita, M. A. 1985, ApJ, 295, L5
———. 1990, in The Interstellar Medium in External Galaxies, ed. H. A. Thronson & J. M. Shull (Dordrecht: Kluwer), 437
Dopita, M. A., & Evans, I. N. 1986, ApJ, 307, 431
Downes, D., & Güsten, R. 1982, Astron. Gesellschaft, 57, 207
Elmegreen, B. G. 1979, ApJ, 231, 372
———. 1982, ApJ, 253, 655
———. 1987, in IAU Symp. 115, Star Forming Regions, ed. M. Peimbert & J. Jugaku (Dordrecht: Reidel), 457
Falgarone, E., & Puget, J. L. 1988, in Galactic and Extragalactic Star Formation, ed. R. E. Pudritz & M. Fich (Dordrecht: Kluwer), 195
Feitzinger, J. V., & Braunsfurth, E. 1984, ApJ, 274, L57

Fich, M., & Tremaine, S. 1991, ARA&A, 29, 409
Field, G. B., Goldsmith, D. W., & Habing, H. J. 1969, ApJ, 155, L149
Field, G. B., & Saslaw, W. C. 1965, ApJ, 142, 568
Franco, J. 1983, ApJ, 264, 508
Franco, J., & Cox, D. P. 1983, ApJ, 273, 243
Freedman, W. L. 1986, in IAU Symp. 166, Luminous Stars and Associations in Galaxies, ed. C. de Loore, A. Willis, & P. Laskarides (Dordrecht: Reidel), 61
Fukui, Y., Sugitani, K., Takaba, H., Iwata, T., Mizuno, A., Ogawa, H., & Kawataba, K. 1986, ApJ, 311, L83
Gordon, M. A., & Burton, W. B. 1976, ApJ, 208, 346
Grabelsky, D. A., Cohen, R. S., Bronfman, L., Thaddeus, P., & May, J. 1987, ApJ, 315, 122
Hamajima, K., & Tosa, M. 1975, PASJ, 27, 561
Iben, I. 1987, private communication
Iben, I., & Tutukov, A. V. 1985, ApJS, 58, 661
Israel, F. P. 1988, in Millimeter and Submillimeter Astronomy, ed. R. D. Wolstencroft & W. B. Burton (Dordrecht, Kluwer), 281
Kennicutt, R. C. 1983, ApJ, 272, 54
————. 1989, ApJ, 344, 685
Kwan, J. 1979, ApJ, 229, 567
Lacey, C. G. 1984, Ph.D. thesis, Univ. Cambridge
Lacey, C. G., & Fall, S. M. 1983, MNRAS, 204, 791
————. 1985, ApJ, 290, 154
Lada, C. J. 1988, in Galactic and Extragalactic Star Formation, ed. R. E. Pudritz & M. Fich (Dordrecht: Kluwer), 5
Larson, R. B. 1972, Nature Phys. Sci., 236, 7
————. 1981, MNRAS, 194, 809
————. 1984, MNRAS, 206, 197
————. 1988, in Galactic and Extragalactic Star Formation, ed. R. E. Pudritz & M. Fich (Dordrecht: Kluwer), 459
Lockman, F. J. 1984, ApJ, 283, 90
Lynden-Bell, D. 1975, Vistas Astron., 19, 299
Madore, B. F. 1977, MNRAS, 178, 1
Maeder, A. 1983, A&A, 120, 149
————. 1987, A&A, 173, 247
Maeder, A., & Meynet, G. 1987, A&A, 182, 243
Maloney, P., & Black, J. H. 1988, ApJ, 325, 389
Mathewson, D. S. 1992, private communication
McCall, M. L., Rybski, P. M., & Shields, G. A. 1985, ApJS, 57, 1
McCray, R. 1988, in Supernova Remnants and the Interstellar Medium, ed. R. S. Roger & T. L. Landecker (Cambridge: Cambridge Univ. Press), 447
McKee, C. F., & Ostriker, J. P. 1977, ApJ, 218, 148
Meatheringham, S. J., Dopita, M. A., Ford, H. C., & Webster, B. L. 1988, ApJ, 327, 651
Miller, G. E., & Scalo, J. M. 1979, ApJS, 41, 513
Mouschovias, T. Ch., Shu, F. H., & Woodward, P. 1974, A&A, 33, 73
Nakai, N., & Sofue, Y. 1982, PASJ, 34, 199
Norman, C., & Silk, J. 1980, ApJ, 238, 158
Penston, M. V., Munday, V. A., Stickland, D. J., & Penston, M. J. 1969, MNRAS, 142, 355
Pettini, M., & West, K. A. 1982, ApJ, 260, 561
Rana, N. C. 1991, ARA&A, 29, 129
Reif, K., Mebold, U., Goss, W. M., van Woerden, H., & Siegman, B. 1982, A&AS, 50, 451
Reynolds, R. J. 1991, ApJ, 372, L17
————. 1992, ApJ, 392, L35
Russell, S. J., & Dopita, M. A. 1992, ApJ, 384, 508
Ryder, S. D. 1993, Ph.D. thesis, Australian National Univ.

Ryder, S. D., & Dopita, M. A. 1993, ApJS, 88, 415
————. 1994, ApJ, 430, 142 (Paper I)
Ryder, S. D., Staveley-Smith, L., Malin, D. F., & Walsh, W. 1994, in preparation
Sanders, D. P., Scoville, N. Z., & Solomon, P. M. 1985, ApJ, 289, 373
Sanders, D. P., Solomon, P. M., & Scoville, N. Z. 1984, ApJ, 276, 182
Sanduleak, N. 1969, AJ, 74, 47
Savage, B. D., & Massa, D. 1985, ApJ, 295, L9
————. 1987, ApJ, 314, 380
Schmidt, M. 1959, ApJ, 129, 243
Scoville, N. Z., & Young, J. S. 1983, ApJ, 265, 148
Searle, L. 1972, in IAU Colloq. 17, L'Age des Etoiles, ed. G. Cayrel de Strobel & A. M. Delplace (Meudon: Obs. Paris), L11
Searle, L., & Sargent, W. L. W. 1972, ApJ, 173, 25
Sellwood, J. A., & Carlberg, R. G. 1984, ApJ, 282, 61
Silk, J. 1985, in IAU Symp. 115, Star Forming Regions, ed. M. Peimbert & J. Jugaku (Dordrecht: Reidel), 663
————. 1988, in Galactic and Extragalactic Star Formation, ed. R. E. Pudritz & M. Fich (Dordrecht: Kluwer), 503
Solomon, P. M., Rivolo, A. R., Barrett, J. W., & Yahil, A. 1987, ApJ, 319, 730
Spicker, J., & Feitzinger, J. V. 1988a, A&A, 191, 10
————. 1988b, A&A, 191, 186
Spitzer, L., & Schwarzschild, M. 1951, ApJ, 114, 106
————. 1953, ApJ, 118, 106
Stark, A. A., & Brand, J. 1989, ApJ, 339, 763
Struck-Marcell, C. 1991, ApJ, 368, 348
Struck-Marcell, C., & Scalo, J. M. 1987, ApJS, 64, 39
Sutherland, R. S., & Dopita, M. A. 1993, ApJS, 88, 253
Talbot, R. J. 1980, ApJ, 235, 821
Talbot, R. J., & Arnett, W. D. 1975, ApJ, 197, 551
Tinsley, B. M. 1980, Fund. Cosmic Phys., 5, 287
Tomisaka, K. 1984, PASJ, 36, 457
————. 1986, PASJ, 38, 95
Tomisaka, K., & Ikeuchi, S. 1986, PASJ, 38, 697
Toomre, A. 1964, ApJ, 139, 121
————. 1981, in The Structure and Evolution of Normal Galaxies, ed. S. M. Fall & D. Lynden-Bell (Cambridge: Cambridge Univ. Press), 111
Twarog, B. A. 1980, ApJ, 242, 242
Vader, J. P., & de Jong, T. 1981, A&A, 100, 124
van der Kruit, P. C., & Searle, L. 1981a, A&A, 95, 105
————. 1981b, A&A, 95, 116
————. 1982, A&A, 110, 61
van der Kruit, P. C., & Shostak, G. S. 1984, A&A, 134, 258
Vassiliadis, E. 1992, Ph.D. thesis, Australian National Univ.
Villumsen, J. V. 1985, ApJ, 290, 75
Wevers, B. M. H. R. 1984, Ph.D. thesis, Univ. Groningen
Wevers, B. M. H. R., van der Kruit, P. C., & Allen, R. J. 1986, A&AS, 66, 505
Wielen, R. 1977, A&A, 60, 263
Wielen, R., & Fuchs, B. 1983, in Kinematics, Dynamics & Structure of the Milky Way, ed. W. L. H. Shuter (Dordrecht: Reidel), 81
Wilson, I. R. G. 1983, Ph.D. thesis, Australian National Univ.
Wyse, R. F. G. 1986, ApJ, 311, L41
Wyse, R. F. G., & Silk, J. 1989, ApJ, 339, 700
Young, J. S. 1988a, in Galactic and Extragalactic Star Formation, ed. R. E. Pudritz & M. Fich (Dordrecht: Kluwer), 579
————. 1988b, in Galactic and Extragalactic Star Formation, ed. R. E. Pudritz & M. Fich (Dordrecht: Kluwer), 611
Young, J. S., & Scoville, N. Z. 1982, ApJ, 258, 467